CHEMSUSCHEM

DOI: 10.1002/cssc.201100443

Homogeneous Catalysis of Valeronitrile Hydrolysis under Supercritical Conditions

Michael Sarlea, Sabine Kohl, Nina Blickhan, and Herbert Vogel*[a]

Supercritical nitrile hydrolysis can be used for both, amide and acid production as well as waste water treatment, as the hydrolysis products show good biodegradability. The conventional process at ambient conditions requires large amounts of mineral acid or base. Approaches that use supercritical water as a green solvent without a catalyst have been investigated over recent years. Findings for valeronitrile hydrolysis presented recently showed promising reaction rates and valeric acid yields. In an attempt to further maximize product yield and to better understand the impact of the pH, reactions in dilute sulfuric acid (0.01 mol$\,L^{-1}$) were performed in a continuous high-pressure laboratory-scale apparatus at 400–500 °C, 30 MPa, and a maximum residence time of 100 s. Results from both reaction media were compared with regard to productivity and sustainability.

Introduction

Organic amides and acids are versatile intermediates used in the chemical and pharmaceutical industries.[1,2] The well-known nitrile hydrolysis process can deliver both products in satisfactory yields if conducted accordingly.[3] However, nitrile hydration usually shows low reaction rates at ambient conditions, and, therefore, strong acids, bases, or enzymes are used as catalysts.[4,5] As a result, large amounts of environmentally unfriendly brine are generated during the extraction of the desired products.[3,6]

Over the last two decades, organic reactions have been performed in supercritical water as it is inexpensive, nonflammable, nontoxic, and abundant.[7–13] In particular, the possibility of tuning properties such as polarity and ionic product by changing the temperature (T) and pressure (p) qualifies supercritical water as an outstanding solvent.[14–20] Usually, hydrolysis reactions are performed at near-critical conditions to take full advantage of the high acidity possessed by water (Figure 1). Furthermore, supercritical water is suitable for reactions that require high temperatures to deliver satisfactory yields. Previous experiments in pure water have demonstrated the remarkable stability of valeronitrile (VN) as significant conversion took place above 400 °C in the given residence time. Nevertheless, significant valeronitrile conversion and valeric acid (VS) selectivity were achieved at high temperatures.[21]

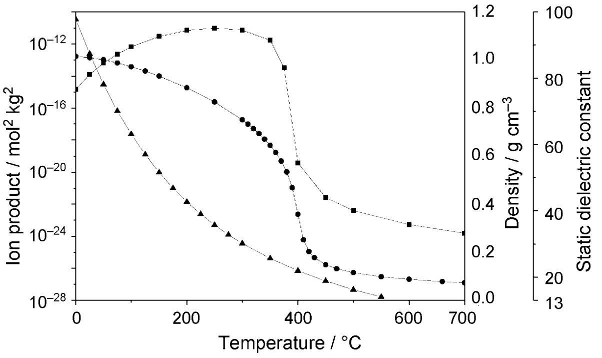

Figure 1. Plot of ion product (■), density (●), and dielectric constant (▲) vs. temperature at $p = 30$ MPa.

An interesting approach is the combination of both methods—hydrolysis of valeronitrile in dilute sulfuric acid under supercritical conditions. Thus, an assessment of homogeneous catalysis on the reaction rates will be performed, which should deliver similar yields and selectivities at shorter reaction times. For a valid comparison, catalyzed kinetic experiments on valeronitrile, valeramide (VA), and valeric acid were performed under the same reaction conditions as the tests performed in pure water.

Kinetic results were gathered and evaluated by using the Presto-Kinetics program. All findings were compared in terms of productivity and sustainability with the results of the reaction in pure water.

Results and Discussion

In general, dissociation above the critical point of water (374 °C, 22 MPa) decreases rapidly with temperature (Figure 1).[22,23] The reduced ability to stabilize ions has been investigated by Xiang et al., who observed a strong dependence between density and dissociation above 350 °C.[24] The low dielectric constant has an impact on salt solubility and polar reaction pathways.[25,26]

Acid-catalyzed nitrile hydrolysis is well-known, and the conventional approach demands 70% sulfuric acid at 100 °C and

---

[a] *Dr. M. Sarlea, Dr. S. Kohl, N. Blickhan, Prof. H. Vogel*
Ernst-Berl-Institut für Technische und Makromolekulare Chemie
Technische Universität Darmstadt
Petersenstrasse 20, 64287 Darmstadt (Germany)
Fax: (+49) 6151-163465
E-mail: vogel@ct.chemie.tu-darmstadt.de

several hours residence time.[3] Similar conversion levels were attained within minutes in pure supercritical water.[21]

The behavior of sulfuric acid under supercritical conditions is quite different compared to that at ambient temperature. The second dissociation constant is very small; thus, the first dissociation reaction may be considered as the only source of hydrogen ions. At comparable conditions of 400 °C and 30 MPa, a dilute sulfuric acid solution of approximately 0.013 $\text{mol}\,\text{L}^{-1}$ exhibits a pH of 3.32.[24]

The reaction pathway consists of the consecutive addition of two water molecules to the nitrile/amide functional group and subsequent ammonia elimination (Scheme 1).[27–29]

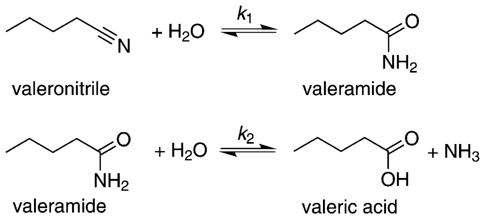

Scheme 1. Valeronitrile hydrolysis pathway via valeramide to yield valeric acid.

The yield of valeric acid was diminished under the aforementioned conditions because of parasitic decarboxylation reactions (Scheme 2).[30,31] As such, the desired outcome of the experiments would be a substantial enhancement of the rate of reaction of the hydrolysis steps along with unchanged or only slightly increased decarboxylation rates. Consequently, higher valeramide and valeric acid yields would be achieved compared to the levels attained in pure supercritical water. Hence, the impact on each reaction step was investigated. The findings are displayed below and start with valeric acid decarboxylation followed by valeramide and valeronitrile hydrolysis.

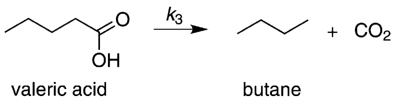

Scheme 2. Decarboxylation of valeric acid to butane and CO_2.

Kinetic analysis and reaction modeling

The reaction equilibria described in the literature were investigated and revealed an insignificant formation of reverse reaction products. Given that water is available in excess, the change in its concentration can be neglected. The level of hydrogen ions remained constant and does not appear in the kinetic equations. Thus, pseudo-first-order reaction kinetics were used to evaluate the experimental data.[32] Furthermore, high amide and acid selectivities occurred without byproduct formation. This allows the evaluation of the kinetic parameters by using a global approach between 400 and 500 °C. The resulting reaction rate constants delivered Arrhenius activation energies and prefactors for each reaction step, which were compared with the data obtained in pure water.

The parameters were modeled by using Presto-Kinetics. The systematic error for plug-flow idealization of tubular-flow reactor data was assessed and resulted in a 2 % deviation, which is low compared to literature values.[33] Both, irreversible and equilibrium reactions between nitrile, amide, and acid were tested, which displayed only slight differences in fit performance. The results with the best fit quality depicted below were obtained with the reaction pathway described in the literature. The degradation products (DP) of valeric acid in the reaction network are shown in Scheme 3.

$$\mathrm{VN}\ \underset{k_{-1}}{\overset{k_1}{\rightleftharpoons}}\ \mathrm{VA}\ \underset{k_{-2}}{\overset{k_2}{\rightleftharpoons}}\ \mathrm{VS}\ \xrightarrow{k_3}\ \mathrm{DP}$$

Scheme 3. Reaction network used to model the experimental data.

The experimental concentration–time data were processed by application of the abovementioned reaction network using the experimental rate constants as starting parameters. The procedure was repeated for all temperature and reactant data sets. A close match between the least-square fit and measured values for all data sets was attained (Figure 2). New reaction rate constants were extracted from the modeled data and used for the Arrhenius activation energy (E_A) calculation and prefactor (A) determination for each reaction step and were compared with the experimental results.

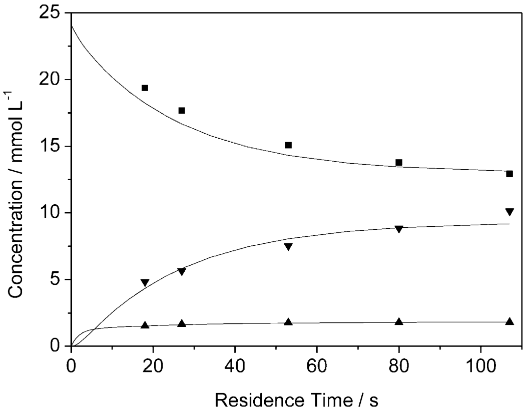

Figure 2. Modeled concentrations and experimental data of valeronitrile (■), valeramide (▲), and valeric acid (▼) hydrolysis at T = 375 °C and p = 30 MPa.

Valeric acid stability

Significant valeric acid conversion takes place above 460 °C in the predetermined residence time. At 460 °C, no difference between the catalyzed and uncatalyzed reaction was observed; at 53 s residence time, 8 % conversion was registered for both media. However, for the same residence time at 500 °C, an increase in conversion of 22 % in water and 28 % in dilute acid was recorded (Figure 3). Thus, the impact on valeric acid decar-

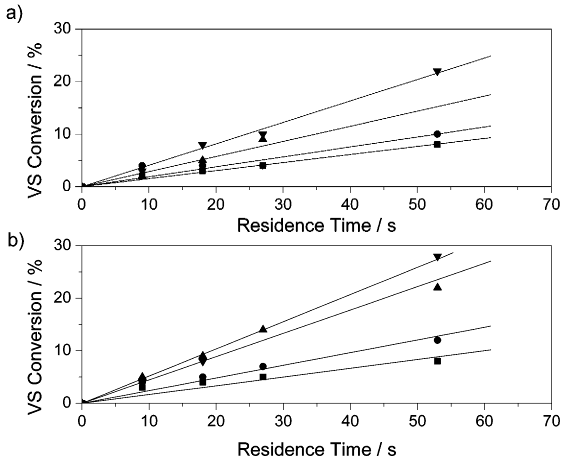

Figure 3. Comparison of valeric acid conversion against residence time at $T = 460$ (■), 475 (●), 490 (▲), and 500 °C (▼), $p = 30$ MPa; concentration of valeronitrile: a) $c = 0.07\ \mathrm{mol\,L^{-1}}$ in water and b) $0.01\ \mathrm{mol\,L^{-1}}$ sulfuric acid.

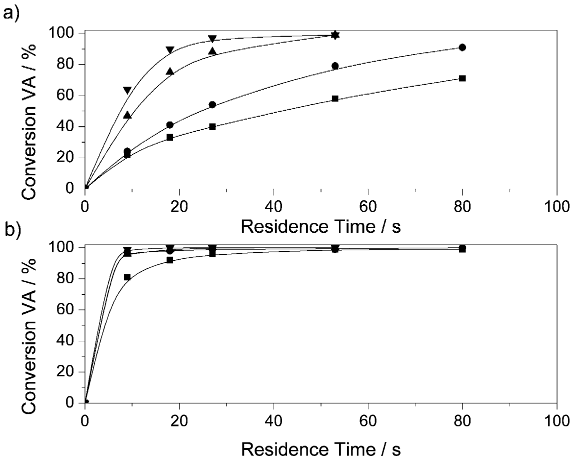

Figure 4. Comparison of valeramide conversion against residence time at $T = 400$ (■), 425 (●), 450 (▲), and 475 °C (▼), $p = 30$ MPa; a) $c = 0.03\ \mathrm{mol\,L^{-1}}$ in water and b) $0.01\ \mathrm{mol\,L^{-1}}$ sulfuric acid.

boxylation is rather small, which is in accordance with the experiments conducted by Belsky et al. on the decarboxylation of acetic acid derivatives.[34]

Both the experimental and modeled activation energies of the catalyzed reaction show an increase of $12\ \mathrm{kJ\,mol^{-1}}$. As both media show similar conversions at low temperatures and by taking into consideration that the temperature has a higher impact on the acid-catalyzed reaction, the resulting activation energy seems plausible. The Arrhenius prefactor is one order of magnitude higher than the prefactor of the uncatalyzed reaction (Table 1).

The findings appear beneficial to preserve high valeric acid yields throughout the given temperature and residence time ranges.

Table 1. Comparison of the activation energies and Arrhenius prefactors obtained from the experimental and modeled data for valeric acid conversion.

Reaction step	E_A [kJ mol^{-1}]		Prefactor A [s^{-1}]	
	experimental	modeled	experimental	modeled
water: VS→DP	143	143	2.03×10^{7}	1.83×10^{7}
acid: VS→DP	155	154	1.70×10^{8}	1.31×10^{8}

Valeramide hydrolysis

Valeramide is an intermediate of the valeronitrile conversion and was separately investigated, as one of the two hydrolysis steps would act as a bottleneck for the consecutive reaction. Valeramide shows higher temperature sensitivity than valeric acid. Reaction conditions were aligned with the previous experiments in pure water. The acid-catalyzed reaction shows considerable enhancement between 400–475 °C (Figure 4). Valeramide conversion reaches 81 % after 9 s at 400 °C, whereas only 24 % conversion is attained in pure water under the same conditions. At higher temperatures, all of the valeramide is consumed within seconds.

Activation energies sustain the high impact of temperature on valeramide hydrolysis in dilute acid. The uncatalyzed reaction displayed a $27\ \mathrm{kJ\,mol^{-1}}$ higher activation energy, and the $42\ \mathrm{kJ\,mol^{-1}}$ difference in the modeled results is even larger (Table 2).

Table 2. Comparison of the activation energies and Arrhenius prefactors obtained from the experimental and modeled data for valeramide hydrolysis.

Reaction step	E_A [kJ mol^{-1}]		Prefactor A [s^{-1}]	
	experimental	modeled	experimental	modeled
water: VA→VS	114	114	1.08×10^{7}	1.03×10^{7}
acid: VA→VS	87	72	4.70×10^{5}	5.21×10^{4}

As expected, a significant increase in valeric acid yield was attained, as the enhancement of the hydrolysis step exceeded the decarboxylation acceleration already presented. Valeramide hydrolysis in pure water resulted in a maximum yield of 90 % valeric acid at 450 °C and 53 s residence time. At higher temperatures, a definite limit to the yield was met owing to the consecutive decarboxylation reaction. In dilute sulfuric acid, higher yields and selectivities were attained, which is remarkable considering the high reaction temperatures. Thus, yields of 99 % valeric acid were recorded after 18 s at 450 °C and after 9 s at 475 °C. At longer residence times, the yields dropped because of the subsequent decarboxylation of valeric acid (Figure 5).

Valeronitrile hydrolysis

The final step concerning the catalytic effect of acid on the reaction pathway is the hydrolysis of valeronitrile. Experiments in pure water showed a higher stability of valeronitrile than valeramide. According to Figure 6, the impact of sulfuric acid on valeronitrile hydrolysis was not as tremendous as it was on valeramide conversion. A considerable effect can be observed at

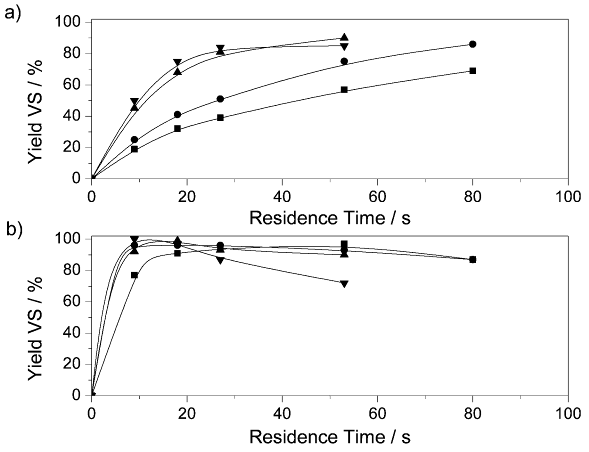

Figure 5. Comparison of valeric acid yield against residence time at $T=400$ (■), 425 (●), 450 (▲), and 475 °C (▼), $p=30$ MPa; concentration of valeramide: a) $c=0.03\ \mathrm{mol\,L^{-1}}$ in water and b) $0.01\ \mathrm{mol\,L^{-1}}$ sulfuric acid.

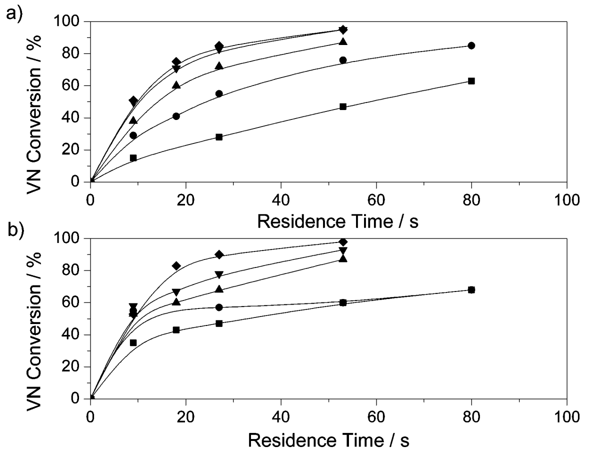

Figure 6. Comparison of valeronitrile conversion against residence time at $T=400$ (■), 425 (●), 450 (▲), 475 (▼), and 500 °C (●), $p=30$ MPa; concentration of valeronitrile: a) $c=0.07\ \mathrm{mol\,L^{-1}}$ in water and b) $0.01\ \mathrm{mol\,L^{-1}}$ sulfuric acid.

low temperatures and short residence times. For instance, a valeronitrile conversion of 15 % at 400 °C after 9 s was recorded, whereas a conversion of 35 % was observed in dilute acid under the same experimental conditions. At higher temperatures and longer residence times, the effect is less significant inasmuch as the enhancement of the conversion remained under 10 %.

The catalytic effect resulted in an activation energy that was approximately 20 kJ mol^{-1} lower (Table 3). Thus, the lower impact compared to valeramide is mirrored by the kinetic results.

A key aspect is the increase in selectivity (Figure 7). After 9 s at 450 °C, a remarkable 98 % valeric acid selectivity was observed. In addition, maximum selectivity shifted to shorter times, especially at temperatures above 450 °C.

However, valeric acid yields attained in dilute sulfuric acid do not exceed the results for pure supercritical water. For example, after 53 s at 450 °C in water, a maximum yield of 80 % was obtained, whereas only 59 % was observed in acid. Nevertheless, a positive impact on valeric acid yields at short residence times over the whole temperature range was noted (Figure 8). In combination with the aforementioned high selectivity, technical applications are conceivable.

Table 3. Comparison of the activation energies and Arrhenius prefactors obtained from the experimental and modeled data for valeronitrile hydrolysis.

Reaction step	E_A [kJ mol^{-1}]		Prefactor A [s^{-1}]	
	experimental	modeled	experimental	modeled
water: VN→VA	98	89	4.81×10^{5}	8.64×10^{4}
acid: VN→VA	79	79	1.70×10^{4}	2.16×10^{4}

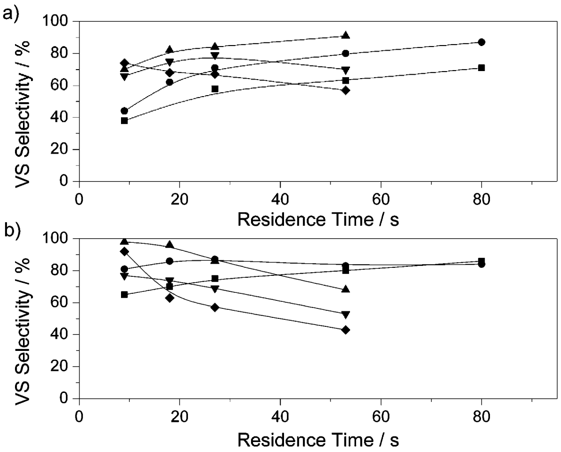

Figure 7. Comparison of valeric acid selectivity against residence time at $T=400$ (■), 425 (●), 450 (▲), 475 (▼), and 500 °C (●), $p=30$ MPa; a) $c=0.07\ \mathrm{mol\,L^{-1}}$ valeronitrile in water and b) $0.01\ \mathrm{mol\,L^{-1}}$ sulfuric acid.

Conclusions

The activation energies extracted from experimental and modeled data exhibit a good correlation. The rates of reaction for hydrolysis and decarboxylation were increased by the addi-

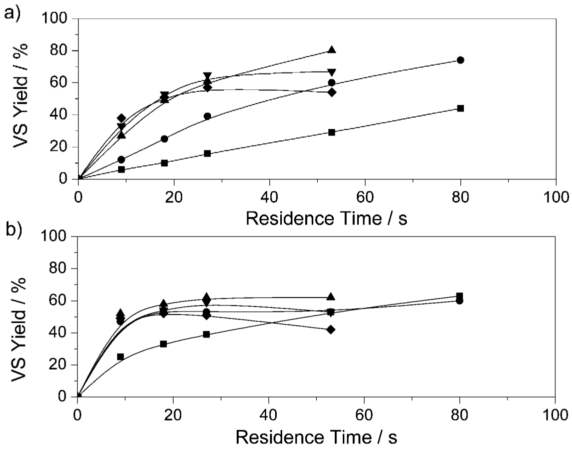

Figure 8. Comparison of valeric acid yield against residence time at $T=400$ (■), 425 (●), 450 (▲), 475 (▼), and 500 °C (◆), $p=30$ MPa; concentration of valeronitrile: a) $c=0.07\ \mathrm{mol\,L^{-1}}$ in water and b) $0.01\ \mathrm{mol\,L^{-1}}$ in sulfuric acid.

tion of sulfuric acid. Nitrile and, in particular, amide hydrolysis show a decrease in activation energy at low pH values. In contrast, decarboxylation exhibits a slight increase; this finding, as well as the calculated activation energies and prefactors, is supported by the literature.[34,35] Experiments conducted with trifluoric acetic and propionic acid exhibit an increase in activation energy of 14–30 kJ mol^{-1} when switching from the anionic to the acidic form. The calculated difference of 12 kJ mol^{-1} matches this trend; the lower margin is caused by the lack of halo groups that stabilize the negative charge on the anion, which results in a lower dissociation constant.

Belsky et al. have performed similar alkyl nitrile hydrolysis experiments [$R{=}CH_3-$, CH_3CH_2-, and $(CH_3)_2CH-$] at near-critical conditions in hydrochloric acid solutions and reported a decrease in activation energy with an increasing electron-donating character of R.[6] The findings presented in this work (79 kJ mol^{-1} for $R{=}CH_3CH_2CH_2-$) match Belsky's trend very well [127, 90, and 83 kJ mol^{-1} for $R{=}CH_3-$, $R{=}CH_3CH_2-$, and $R{=}(CH_3)_2CH-$, respectively].

The impact of a low sulfuric acid concentration on the conversion of valeronitrile in supercritical water has to be evaluated by taking each reaction step into consideration. Although the nitrile conversion rate was only increased at low temperatures with acid addition, a significant increase in selectivity was attained for short residence times.

The substantial enhancement of valeramide conversion was observed, which is supported by the calculated activation energies. The valeric acid yields reached 99 %, which is a remarkable improvement considering the short residence times in comparison to the levels attained in pure water. As only a little acid was required, the amounts of waste salt produced during product purification should be acceptable from a technical point of view. However, even low concentrations of sulfuric acid enhance corrosion because sulfate anions act as oxidants in high-temperature water.[36] The impact is particularly distinct at temperatures around 200 °C and results in a potential homogeneous active dissolution of the reactor material, which occurs during heat-up or cool-down of the reaction solution.[37] At higher temperatures, passivation of the alloy takes place.[38] It might be beneficial to switch to phosphorous acid as a catalyst because it exhibits less aggressive properties at low concentrations. Conversely, reactor plugging attributable to poorly soluble phosphates can occur.[36]

Almost no catalytic impact was observed for valeric acid decarboxylation, which is a positive result, as no acceleration of the degradation of the commercial product occurs.

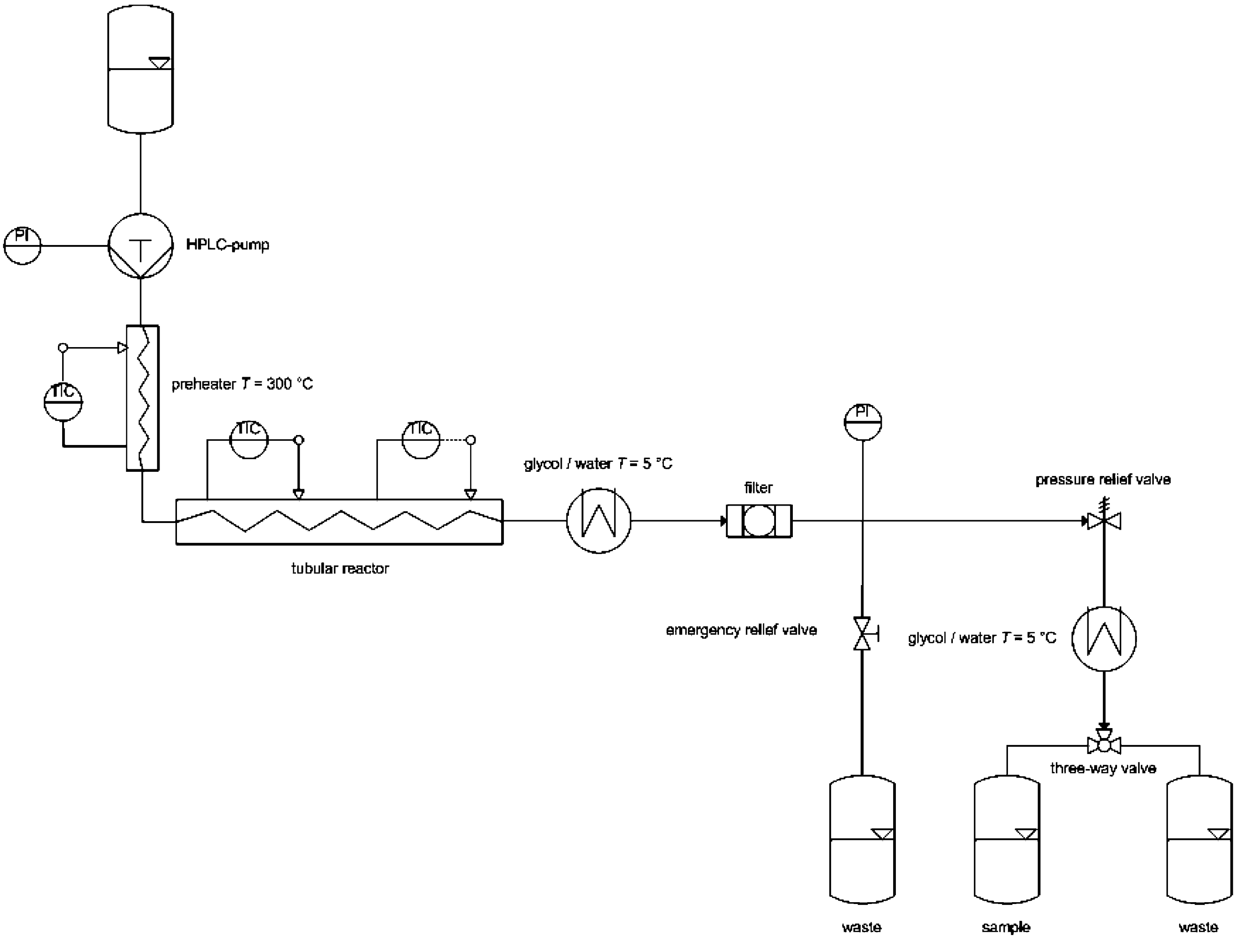

Scheme 4. Schematic representation of the high-pressure plant used for nitrile hydrolysis under supercritical conditions.

The overall yield of valeric acid was not improved significantly; hence, pure supercritical water would still be the preferred solvent for industrial scale-up. The key benefit is a lower environmental impact, as no waste brine is generated. Furthermore, corrosion issues, which could be induced by sulfuric acid, and potential plugging caused by salts with poor solubility are avoided. Sulfate ions, which are not considered as an oxidizing agent at room temperature, may act as strong oxidizers in high-temperature water. Thereby, metals might undergo fast active dissolution.[36] Nickel-based alloys are widely used for high-temperature applications under corrosive conditions. These materials are attacked by most acidic solutions of high density, regardless if sub- or supercritical. However, their corrosion rates are low in low-density supercritical solutions; hence, a reactor made from these alloys is conceivable. However, preheat and cool-down sections should be made from a different material. Niobium and tantalum are resistant to H_2SO_4 solutions below approximately 350 °C.[39]

Nevertheless, the addition of catalytic amounts of acid is reasonable, if valeric acid is produced directly from valeramide because of a significant impact on reaction rates as well as increased yields and valeric acid selectivities.

Experimental Section

Testing plant

The schematic setup of the high-pressure plant is shown in Scheme 4. The feed was pumped through the preheater into the reactor by using an HPLC pump. The tubular reactor was made of Inconel C276 (2.83 cm^3 volume) and was spirally embedded into an aluminum cylinder. The cylinder was enfolded by using an aluminum coat and heated by using a 500 W heating device. After passing the reactor, the reaction mixture was cooled down and depressurized. The plant was designed for a maximum temperature of 560 °C and a pressure of 40 MPa. Residence times between 8–120 s were adjusted by flow variation.

Analysis

The reaction mixture was analyzed by using GC [SHIMADZU GC-17 A, capillary column (CW 20M MN Fused Silica, $L=19$ m, inner diameter (*ID*): 0.32 mm, $d_f=0{,}5$ μm), nitrogen as carrier gas, flame ionization detector] and HPLC [KNAUER HPLC equipped with a Knauer smartline RI detector 2300 and a Knauer smartline UV detector 2500 (@210 nm), column (ProntoSIL C18 ACE-EPS, $L=250$ mm, $ID=3$ mm, particle size = 3.0 μm) and 2.5 mM sulfuric acid in 9:1 water/acetonitrile as eluent].
Chemicals: valeronitrile (technical grade, purchased from Lonza), valeramide (97 %, Acros), and valeric acid (99 %, Acros).

Acknowledgements

The authors would like to thank Lonza AG, Visp, for their financial support of this work.

Keywords: homogeneous catalysis · hydrolysis · kinetics · supercritical fluids · sustainable chemistry

[1] B. Izzo, C. L. Harrell, M. T. Klein, *AIChE J.* **1997**, *43*, 2048 – 2058.
[2] H. Römpp, J. Falbe, M. Regitz, *RÖMPP Chemie Lexikon* 9th Ed., Thieme Verlag, Stuttgart, **1996**.
[3] R. M. Lincoln (Atlantic Richfield Company), US 3876691 A, **1975**.
[4] M. Ress-Loeschke, B. Hauer, R. Mattes, D. Engels (BASF AG), DE 10010149, **2003**.
[5] C. O'Reilly, P. D. Turner, *J. Appl. Microbiol.* **2003**, *95*, 1161 – 1174.
[6] A. J. Belsky, T. B. Brill, *J. Phys. Chem. A* **1999**, *103*, 3006 – 3012.
[7] B. Subramaniam, M. A. McHugh, *Ind. Eng. Chem. Process Des. Dev.* **1986**, *25*, 1 – 12.
[8] M. Perrut, *Ind. Eng. Chem. Res.* **2000**, *39*, 4531 – 4535.
[9] A. R. Katritzky, D. A. Nichols, M. Siskin, R. Murugan, M. Balasubramanian, *Chem. Rev.* **2001**, *101*, 837 – 892.
[10] P. E. Savage, S. Gopalan, T. I. Mizan, C. J. Martino, E. E. Brock, *AIChE J.* **1995**, *41*, 1723 – 1778.
[11] H. Weingärtner, E. U. Franck, *Angew. Chem.* **2005**, *117*, 2730 – 2752; *Angew. Chem. Int. Ed.* **2005**, *44*, 2672 – 2692.
[12] P. G. Jessop, W. Leitner, *Chemical Synthesis Using Supercritical Fluids* (Eds.: P. G. Jessop, W. Leitner), Wiley-VCH, Weinheim, **1999**, Chapter 1.
[13] S. E. Hunter, P. E. Savage, *Chem. Eng. Sci.* **2004**, *59*, 4903 – 4909.
[14] E. Dinjus, R. Fornika, M. R. Scholz, *Chemistry under Extreme or Non-Classical Conditions*, 1st Ed. (Eds.: R. van Eldik, C. D. Hubbard), Wiley-VCH, Weinheim, **1996**, Chapter 6.
[15] X.-Y. Zheng, Y. Arai, T. Furuya, *Trends Chem. Eng.* **1996**, *3*, 205 – 217.
[16] N. Akiya, P. E. Savage, *Chem. Rev.* **2002**, *102*, 2725 – 2750.
[17] A. Kruse, E. Dinjus, *J. of Supercritical Fluids* **2007**, *39*, 362 – 380.
[18] S. Mittelstädt, *Anwendung der Chemie unter überkritischen Bedingungen auf technisch interessante Synthesen*, Dissertation, Technische Universität Darmstadt (D), **1997**.
[19] S. D. Iyer, M. T. Klein, *J. of Supercritical Fluids* **1997**, *10*, 191 – 200.
[20] B. Izzo, M. T. Klein, *Ind. Eng. Chem. Res.* **1999**, *38*, 1183 – 1191.
[21] M. Sarlea, S. Kohl, N. Blickhan, H. Vogel, *ChemSusChem* **2010**, *3*, 85 – 90.
[22] M. Uematsu, E. U. Frank, *J. Phys. Chem. Ref. Data* **1980**, *9*, 1291 – 1306.
[23] W. L. Marshall, E. U. Frank, *J. Phys. Chem. Ref. Data* **1981**, *10*, 295 – 304.
[24] T. Xiang, K. P. Johnston, W. T. Wofford, E. F. Gloyna, *Ind. Eng. Chem. Res.* **1996**, *35*, 4788 – 4795.
[25] F. J. Armellini, J. W. Tester, *J. Supercrit. Fluids* **1991**, *4*, 254 – 264.
[26] F. J. Armellini, J. W. Tester, *J. Supercrit. Fluids* **1994**, *7*, 147 – 158.
[27] J. Clayden, N. Greeves, S. Warren, P. Wothers, *Organic Chemistry*, Oxford University Press, Oxford, **2001**.
[28] R. Brückner, *Reaktionsmechanismen* 2nd Ed., Spektrum Akademischer Verlag, Heidelberg, **2002**.
[29] L. A. M. M. Barbosa, R. A. van Santen, *J. Mol. Catal. A: Chem.* **2001**, *166*, 101 – 121.
[30] S. Matsubara, Y. Yokota, K. Oshima, *Org. Lett.* **2004**, *6*, 2071 – 2073.
[31] M. Okazaki, T. Funazukuri, *J. Mater. Sci.* **2006**, *41*, 1517 – 1521.
[32] N. A. Bhore, M. T. Klein, K. B. Bischoff, *Ind. Eng. Chem. Res.* **1990**, *29*, 313 – 316.
[33] S. V. Ramayya, M. J. Antal, *Energy Fuels* **1989**, *3*, 105 – 108.
[34] A. J. Belsky, P. G. Maiella, T. B. Brill, *J. Phys. Chem. A* **1999**, *103*, 4253 – 4260.
[35] D. Miksa, J. Li, T. B. Brill, *J. Phys. Chem. A* **2002**, *106*, 11107 – 11114.
[36] P. Kritzer, *J. Supercrit. Fluids* **2004**, *29*, 1 – 29.
[37] P. Kritzer, N. Boukis, E. Dinjus, *Corrosion* **1998**, *54*, 689 – 699.
[38] P. Kritzer, N. Boukis, E. Dinjus, *Corrosion* **2000**, *56*, 1093 – 1104.
[39] P. Kritzer, N. Boukis, E. Dinjus, *J. Supercrit. Fluids* **1999**, *15*, 205 – 227.

Received: August 9, 2011